THE SPECTROSCOPIC ORBITS OF FIVE SOLAR-TYPE, SINGLE-LINED BINARIES

Francis C. Fekel[1], Samira Rajabi, Matthew W. Muterspaugh, and Michael H. Williamson

Center of Excellence in Information Systems, Tennessee State University, 3500 John A. Merritt Boulevard, Box 9501, Nashville, TN 37209, USA;
fekel@evans.tsuniv.edu, samira@coe.tsuniv.edu, matthew1@coe.tsuniv.edu, michael.h.williamson@gmail.com

ABSTRACT

We have determined spectroscopic orbits for five single-lined spectroscopic binaries, HD 100167, HD 135991, HD 140667, HD 158222, HD 217924. Their periods range from 60.6 to 2403 days and the eccentricities from 0.20 to 0.84. Our spectral classes for the stars confirm that they are of solar type, F9–G5, and all are dwarfs. Their [Fe/H] abundances, determined spectroscopically, are close to the solar value and on average are 0.12 greater than abundances from a photometric calibration. Four of the five stars are rotating faster than their predicted pseudosynchronous rotational velocities.

Key words: binaries: spectroscopic – stars: abundances – stars: individual (HD 100167, HD 135991, HD 140667, HD 158222, HD 217924)

Online-only material: machine-readable and VO tables

1. INTRODUCTION

Nearly a decade ago a group of solar-type stars with *V* magnitudes between 5.9 and 8.1 was selected to expand a photometric program that was designed to detect long-term spot cycles in dwarfs similar to the Sun (Henry 1999). Although most of these moderately bright stars had radial velocities published in the literature, many did not. To remove binaries from the photometric sample, we obtained spectra and measured radial velocities. Our spectroscopic observations soon identified five single-lined binaries, HD 100167, HD 135991, HD 140667, HD 158222, and HD 217924, which we continued to observe. The basic properties of these binaries are given in Table 1. During the course of our extended spectroscopic observing campaign, others have also identified these five stars as binaries. From our observations we determine spectroscopic orbits and spectral and luminosity classes, measure iron abundances and *v* sin *i* values, and then briefly discuss the systems.

2. OBSERVATIONS AND RADIAL VELOCITIES

From 2002 through 2012 we obtained observations at the Kitt Peak National Observatory (KPNO) with the coudé feed telescope and coudé spectrograph. The vast majority were acquired with a TI CCD detector, and those spectrograms were centered at 6430 Å, cover a wavelength range of 84 Å, and have a resolution of 0.21 Å or a resolving power of just over 30,000. The TI CCD was unavailable in 2008 September, and so a Tektronics CCD, designated T1KA, was used instead. With that CCD the spectrum was centered at 6400 Å. Although the wavelength range covered by the chip increased to 172 Å, the resolving power decreased to 19,000. Beginning in 2010 September we acquired spectra with a CCD, consisting of a 2600 × 4000 array of 12 μm pixels, that was made by Semiconductor Technology Associates and designated STA2. With STA2 the spectrum was once again centered at 6430 Å, and the much larger size of the detector produced a wavelength range of 336 Å. The spectrograph slit was set so that the STA2

spectra have the same resolution as those acquired with the TI CCD although there is some worsening of the resolution at both ends of the STA2 spectra. All our KPNO spectra have signal-to-noise (S/N) ratios of about 150.

Starting in 2006, we collected additional spectrograms with the Tennessee State University (TSU) 2 m automatic spectroscopic telescope (AST) and a fiber-fed echelle spectrograph, situated at Fairborn Observatory near Washington Camp in the Patagonia Mountains of southeastern Arizona (Eaton & Williamson 2004, 2007). Through 2011 June the detector was a 2048 × 4096 SITe ST-002A CCD with 15 μm pixels. Eaton & Williamson (2007) have discussed reduction of the raw spectra and their wavelength calibration. The AST echelle spectrograms have 21 orders that cover the wavelength range 4920–7100 Å, and most have an average resolution of 0.17 Å although a few have a slightly lower resolution of 0.24 Å. The S/N ratios ranged from 30 to 80, being affected in part by significant temperature fluctuations of the dewar.

Beginning in 2010 January, we made several upgrades to the TSU 2 m AST to increase throughput, sensitivity, and flexibility. First, an entirely new focal plane assembly and guide system were constructed and installed, including a replacement for the fiber optic links between the telescope's focal plane and spectrographs. The new system increases the number of available fibers from 3 to a maximum of 12, each terminated with industry-standard SMA connectors, and enables the switching between fibers to occur in a matter of seconds. This configuration expands our flexibility and allows us to host guest instruments. The fibers connect to custom one-inch aluminum mirrors, and the connector tine is flush with the front mirror surface. A nonpolarizing cubic customized 70/20 beam splitter is placed before the mirror/fiber tip to redirect the smaller portion of starlight to a small CCD camera for direct guiding; starlight reflected back from the mirror/fiber connector is redirected by the beam splitter in the opposite direction, where a second CCD camera can similarly be used as a "slit monitor" and for guiding on brighter stars. Second, an aluminum secondary mirror replaced the telescope's existing metal mirror, because the latter's protective coating had very significantly eroded with time. Third, in the summer of 2011 the SITe CCD detector and dewar were replaced with a Fairchild 486 CCD having 4K × 4K 15 μm pixels, which required a new readout electronics package,

---

[1] Visiting Astronomer, Kitt Peak National Observatory, National Optical Astronomy Observatory, operated by the Association of Universities for Research in Astronomy, Inc., under cooperative agreement with the National Science Foundation.

Table 1
Basic Properties

HD	HIP	V^a (mag)	$B-V^a$ (mag)	Parallax[b] (mas)
100167	56257	7.35	0.617	28.26 ± 0.72
135991	74821	7.84	0.578	19.56 ± 0.91
140667	77098	7.53	0.611	30.39 ± 1.54
158222	85244	7.82	0.667	24.05 ± 0.65
217924	113884	7.22	0.631	38.37 ± 2.11

Notes.
[a] Perryman et al. (1997).
[b] van Leeuwen (2007).

Table 3
Spectral Type and $v \sin i$

HD	Spectral Type[a]	$v \sin i$ (km s^{-1})
100167	G0 dwarf	3.2
135991	F9 dwarf	6.7
140667	F9 dwarf	2.3
158222	G5 V	2.2
217924	G2 V	2.2

Note.
[a] dwarf = luminosity classification from comparison of absolute magnitude with canonical value rather than from the spectrum itself.

and a new dewar with a Cryotiger refrigeration system, which is consistently cooled at −110 °C. Overall, these improvements have increased the throughput by at least a factor of 30. The echelle spectrograms that were obtained with this new detector have 48 orders, covering the wavelength range 3800–8260 Å. Because different diameter fibers were used at times, the resolution was either 0.24 or 0.4 Å, which resulted in S/N ratios that ranged from 60 to 130 at 6000 Å. Finally, a new temperature controlled building has been constructed to host guest instruments. It has two rooms, one, which measures 6 ft by 30 ft, to house the electronics systems and a second, which is 11 ft by 30 ft, to accommodate optics systems.

The KPNO velocities were determined by cross-correlation with respect to IAU radial velocity standard stars of similar spectral type, β Vir, HR 7560, and ι Psc. The velocities adopted for those standards are from Scarfe (2010).

Fekel et al. (2009) described the measurement of the radial velocities from the Fairborn Observatory AST spectra. Unlike the KPNO velocities those from Fairborn Observatory are absolute velocities. Our unpublished velocities of several IAU solar-type standard stars indicate that the Fairborn Observatory velocities taken with the SITe CCD have a small zero-point offset of −0.3 km s^{-1} relative to the velocities of Scarfe (2010). Starting in the fall of 2011, velocities from spectra obtained with the new CCD system have a zero-point offset −0.6 km s^{-1} relative to those of Scarfe (2010). Thus, we added either 0.3 or 0.6 km s^{-1}, depending on which detector was used, to each measured velocity so that the zero point of the Fairborn velocities is the same as that of the KPNO velocities.

3. GENERAL ORBITAL ANALYSIS

For each of the five stars we first found a preliminary orbital period with the program PDFND, which uses the least string

method, implemented by T. J. Deeming (Bopp et al. 1970), to identify the period. We then computed a preliminary orbit for each star with the program BISP (Wolfe et al. 1967), which uses a slightly modified version of the Wilsing–Russell method. We refined those orbits with SB1 (Barker et al. 1967), a program that computes differential corrections.

For each star we determined separate solutions of the KPNO velocities and the Fairborn Observatory velocities. From the ratio of the variances of the solutions, we then determined weights for the velocities from the two observatories and produced a final orbital solution, listed in Table 2, with the combined set of velocities.

4. SPECTRAL TYPE

Strassmeier & Fekel (1990) identified several luminosity-sensitive and temperature-sensitive line ratios in the 6430–6465 Å region. They employed those critical line ratios and the general appearance of the spectrum as spectral-type criteria. However, for stars that are hotter than about early-G spectral class, the line ratios in that wavelength region have little sensitivity to luminosity. In those cases we have used the entire 84 Å spectral region of our KPNO observations to estimate just the spectral classes of the individual components. The luminosity class may be determined by computing the absolute visual magnitude with the *Hipparcos* parallax and comparing that magnitude to evolutionary tracks or a table of canonical values for giants and dwarfs. Such a luminosity class that is not derived from the actual spectrum we note as "dwarf" rather than with the Roman numeral luminosity class. Our classifications are summarized in Table 3.

Table 2
Orbital Elements and Related Parameters

HD	P (days)	T (HJD)	e	ω (deg)	K (km s^{-1})	γ (km s^{-1})	$a \sin i$ (10^6 km)	$f(m)$ ($M_\odot$)
100167	60.58037	2454239.1125	0.67827	20.661	26.975	−20.218	16.512	0.04900
	±0.00030	±0.0067	±0.00047	±0.072	±0.029	±0.013	±0.020	±0.00018
135991	151.0054	2454262.42	0.5697	135.44	8.057	−24.916	13.749	0.004542
	±0.0094	±0.11	±0.0022	±0.40	±0.027	±0.020	±0.053	±0.000052
140667	978.42	2454060.0	0.2040	202.1	4.725	−16.727	62.23	0.01003
	±0.94	±3.2	±0.0049	±1.2	±0.022	±0.015	±0.30	±0.00014
158222	206.088	2454309.15	0.4126	78.94	10.994	−25.549	28.380	0.02145
	±0.018	±0.16	±0.0017	±0.30	±0.022	±0.015	±0.062	±0.00014
217924	2402.7	2455181.29	0.8449	58.16	6.778	16.572	119.8	0.01187
	±17.7	±0.67	±0.0036	±0.53	±0.057	±0.017	±1.9	±0.00049

5. PROJECTED ROTATIONAL VELOCITY

We have determined $v \sin i$ values from our red-wavelength KPNO spectra with the procedure of Fekel (1997). Following Fekel (1997), for late-F and G stars, we adopted a macroturbulent broadening value of 3 km s^{-1}. The resulting projected rotational velocities are listed in Table 3. Those $v \sin i$ values have estimated uncertainties of 1 km s^{-1}.

6. ABUNDANCE ANALYSIS

We determined the iron abundance for each of the five stars from our Fairborn Observatory echelle spectra. Our line list was taken from Bubar & King (2010) and includes between 34 and 45 Fe I lines for each star. All abundances were derived from equivalent width (EW) measurements with the use of the IRAF splot package. Table 4 shows the line list for each star along with the excitation potential (EP), oscillation strength (log gf), and measured width for each line. We obtained stellar model atmospheres for the stars by interpolating non-overshoot models in the ATLAS9 grid (Castelli & Kurucz 2003). The initial effective temperature $T_{\rm eff}$ and log gf values are from Casagrande et al. (2011). We adopted the solar abundance of iron as the starting value in the atmospheric model for each star and chose an initial microturbulent velocity, v_t, of 1.5 km s^{-1}. We used the model atmosphere as input to the LTE line abundance analysis code MOOG, developed by Sneden (1973). We then refined the parameters iteratively until there was no trend in Fe I abundance as a function of reduced equivalent width or as a function of EP. An increase of 100 K in the adopted temperature increases the abundance by 0.06 dex. The best-fit model parameters for each star and the derived [Fe/H] abundances and standard deviation (σ) values are listed in Table 5.

6.1. Results Comparison

All five of our binaries are included in the Geneva–Copenhagen survey of solar neighborhood stars (Nordström et al. 2004), which provided basic properties, including abundance estimates. Holmberg et al. (2007) derived an improved photometric iron abundance calibration using Strömgren photometry and redetermined the iron abundances for the stars in that survey. In Table 6 we compare their adopted effective temperatures and revised [Fe/H] values with our results. On average our effective temperatures are 155 ± 18 K higher resulting in the [Fe/H] values being 0.12 ± 0.03 greater than those of Holmberg et al. (2007). One of our binaries, HD 100167, has a previously determined spectroscopic iron abundance. Valenti & Fischer (2005) found $T_{\rm eff} = 5915$ K and [Fe/H] = 0.06 for that star, values which are essentially identical to ours.

7. CIRCULARIZATION AND SYNCHRONIZATION

The two main theories of orbital circularization and rotational synchronization (e.g., Zahn 1977; Tassoul & Tassoul 1992) disagree significantly on absolute time scales but do agree that synchronization should occur first. Observationally, Duquennoy & Mayor (1991) examined the multiplicity of solar-type stars in the solar neighborhood. They determined that while systems with periods ⩽10 days had circular orbits, longer period orbits are generally eccentric. With periods ranging from 60.6 to 2403 days it is not surprising that the five binaries have significant eccentricities, which range from 0.20 for HD 140667 to 0.845 for HD 217924.

Obviously, in an eccentric orbit true synchronization can not occur. However, for a non-circular orbit Hut (1981) has shown that the rotational angular velocity of a star will tend to synchronize with that of the orbital motion at periastron, a condition called pseudosynchronization. With Equation (42) of Hut (1981), we compute pseudosynchronous periods of 10.4, 41.8, 781.6, 97.0, and 132.2 days for HD 100167, HD 135991, HD 140667, HD 158222, and HD 217924, respectively.

8. INDIVIDUAL STARS

8.1. HD 100167 = HIP 56257

8.1.1. Brief History

Nidever et al. (2002) included HD 100167 [$\alpha = 11^{\rm h}31^{\rm m}53\overset{\rm s}{.}91$ $\delta = 41°26'21\overset{''}{.}8$ (2000)] in a velocity survey of late-type stars. From two observations they found it to have a variable velocity with an average of −27.6 km s^{-1}. Nordström et al. (2004) listed HD 100167 in another extensive compilation, the Geneva–Copenhagen survey of solar neighborhood stars. From two Coravel observations they determined an average velocity of −28.1 km s^{-1} and also identified the star as a binary. HD 100167 was initially considered for the Keck planet search program, and from a single spectrogram Valenti & Fischer (2005) found a velocity of −29.5 km s^{-1}. White et al. (2007) observed HD 100167 twice as part of yet another survey. Their work supported the *Spitzer* Legacy Science Program "Formation and Evolution of Planetary Systems." Velocities of their two spectra differ by 3.4 km s^{-1} but have an average velocity of −27.3 km s^{-1}, similar to previous results.

Both Nordström et al. (2004) and Valenti & Fischer (2005) determined the metallicity and rotational velocity of HD 100167. Nordström et al. (2004) found [Fe/H] = −0.05, revised by Holmberg et al. (2007) to −0.09, and $v \sin i = 5$ km s^{-1}, while Valenti & Fischer (2005) got [Fe/H] = 0.06 and $v \sin i = 3.8$ km s^{-1}.

Based on a comparison with a grid of stellar evolutionary tracks, Holmberg et al. (2009) determined an age of 6.8 Gyr for HD 100167, while Takeda et al. (2007) found a likely age of 3.4 Gyr. Wright et al. (2004) obtained Ca II H and K emission measurements from high resolution spectra and determined an age of 2.3 Gyr. From the more recent activity–age calibration of Mamajek & Hillenbrand (2008, their Equation (3)) the age is slightly increased to 2.7 Gyr. Also using stellar activity indicators, Carpenter et al. (2009) assigned a younger age of 1.58 Gyr for HD 100167.

8.1.2. Orbital Analysis

With 142 Fairborn Observatory velocities all phases of the very eccentric orbit of HD 100167 are well sampled. However, our 23 KPNO radial velocities only partly cover the orbit with much of the very eccentric portion of the velocity curve missing. Thus, in computing an orbit for the KPNO velocities we fixed the semiamplitude at the value from the Fairborn Observatory solution. The center-of-mass velocities of the Fairborn and KPNO solutions differ by just 0.1 km s^{-1}, and the other elements are also in very good agreement, so we combined the two data sets, assigning weights of 1.0 and 0.15 to the Fairborn and KPNO velocities, respectively, and computed a final orbital solution. Table 7 provides a list of our velocities, and the final orbital elements from the joint data solution are given in Table 2. Figure 1 compares the velocities with the radial velocity curve computed from the final orbital elements.

Table 4
Equivalent Widths

Wavelength	EP	$\log gf$	Equivalent Width				
(Å)	(eV)		HD 100167	HD 135991	HD 140667	HD 158222	HD 217924
5522.45	4.21	−1.55	41.2	. . .	32.0	45.9	27.9
5539.28	3.64	−2.66	. . .	. . .	8.9	. . .	11.5
5543.94	4.22	−1.14	. . .	. . .	47.9	62.4	. . .
5546.50	4.37	−1.31	. . .	. . .	36.4	. . .	. . .
5546.99	4.22	−1.91	. . .	. . .	12.9	. . .	41.1
5554.88	4.55	−0.44	94.3	76.8	76.3	106.5	78.9
5560.21	4.43	−1.19	46.5	. . .	31.5	. . .	. . .
5576.09	3.43	−1.00	113.2	92.5	97.4	113.6	98.4
5679.02	4.65	−0.92	. . .	. . .	41.2	. . .	. . .
5717.83	4.28	−1.13	. . .	54.4	37.7	66.0	59.5
5731.76	4.26	−1.30	. . .	. . .	38.8	. . .	46.8
5732.27	4.99	−1.56	. . .	. . .	3.7	. . .	. . .
5741.85	4.26	−1.85	. . .	21.1	. . .	. . .	27.7
5752.03	4.55	−1.18	51.2	43.0	43.2	54.7	32.7
5775.08	4.22	−1.30	. . .	. . .	46.5	55.8	52.4
5778.45	2.59	−3.48	. . .	. . .	. . .	. . .	12.7
5905.67	4.65	−0.73	56.2	48.3	39.8	61.0	37.0
5916.25	2.45	−2.99	54.2	. . .	36.8	54.5	38.8
5927.79	4.65	−1.09	40.6	27.2	26.1	42.4	34.4
5929.68	4.55	−1.41	38.0	23.0	. . .	. . .	. . .
5930.17	4.65	−0.23	90.4	85.2	. . .	. . .	82.3
5934.65	3.93	−1.17	. . .	64.7	. . .	. . .	66.2
5956.69	0.86	−4.60	44.1	. . .	33.6	. . .	34.7
6003.01	3.88	−1.12	67.5	. . .	64.8	75.6	73.8
6027.05	4.08	−1.09	59.7	56.2	46.8	67.5	42.8
6055.99	4.73	−0.46	67.1	59.7	. . .	. . .	50.8
6065.48	2.61	−1.53	112.1	99.6	. . .	. . .	100.2
6078.49	4.80	−0.32	75.1	. . .	58.6	80.7	58.8
6079.00	4.65	−1.12	40.5	. . .	29.4	40.5	27.0
6127.91	4.14	−1.40	. . .	. . .	33.0	. . .	36.1
6151.62	2.18	−3.30	47.6	. . .	31.1	48.9	34.2
6159.37	4.61	−1.97	10.8	. . .	. . .	. . .	. . .
6165.36	4.14	−1.47	38.1	28.6	25.5	44.7	31.1
6173.34	2.22	−2.88	. . .	51.4	53.1	. . .	63.0
6187.99	3.94	−1.72	41.3	. . .	. . .	49.0	. . .
6213.43	2.22	−2.48	70.8	58.2	71.1	. . .	68.4
6219.28	2.20	−2.43	80.3	69.8	75.9	86.9	70.4
6246.32	3.60	−0.73	. . .	99.1	. . .	. . .	94.7
6252.55	2.40	−1.69	117.3	103.9	97.7	116.3	. . .
6265.13	2.17	−2.55	78.6	66.9	65.7	85.6	75.8
6271.28	3.33	−2.72	. . .	. . .	. . .	21.1	. . .
6290.97	4.73	−0.78	. . .	72.9	. . .	. . .	. . .
6293.92	4.83	−1.72	38.7	. . .	. . .	51.3	. . .
6322.68	2.59	−2.43	. . .	54.9	59.6	. . .	53.0
6335.33	2.20	−2.18	92.5	76.5	84.4	95.6	86.2
6336.82	3.68	−0.91	101.9	91.3	87.0	107.1	90.8
6344.15	2.43	−2.92	. . .	. . .	46.7	64.9	48.8
6380.74	4.19	−1.38	50.1	33.1	40.2	. . .	. . .
6393.61	2.43	−1.57	120.6	98.8	104.5	127.6	107.8
6469.19	4.83	−0.77	45.5	. . .	40.2	55.2	56.0
6533.94	4.56	−1.38	29.0	19.0	. . .	33.0	. . .
6591.31	4.59	−2.07	. . .	. . .	. . .	14.8	. . .
6593.87	2.43	−2.42	77.2	66.8	66.2	88.8	79.9
6597.56	4.79	−1.07	41.8	33.7	31.5	44.6	37.4
6608.02	2.28	−4.03	13.9	. . .	. . .	24.9	. . .
6677.99	2.69	−1.35	126.6	97.1	106.2	116.1	102.6
6703.57	2.76	−3.16	34.9	16.8	20.5	40.0	. . .
6710.32	1.49	−4.88	. . .	. . .	. . .	18.7	. . .
6715.38	4.61	−1.64	24.6	18.8	. . .	30.8	. . .
6716.22	4.58	−1.92	13.5	8.0	9.4	15.3	. . .
6725.35	4.10	−2.30	. . .	. . .	. . .	16.5	14.1
6726.67	4.61	−1.13	44.5	36.0	29.5	47.6	37.3
6750.15	2.42	−2.62	68.8	55.5	53.8	72.5	63.5
6752.72	4.64	−1.30	. . .	13.0	. . .	. . .	30.7

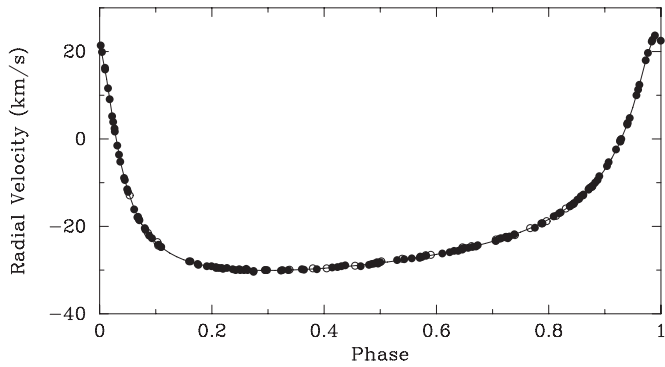**Note.** Equivalent widths are given in units of mÅ.

Figure 1. Radial velocities of HD 100167 compared with the computed velocity curve. Dots: Fairborn Observatory; open circles: KPNO. Zero phase is a time of periastron passage.

Figure 2. Radial velocities of HD 135991 compared with the computed velocity curve. Dots: Fairborn Observatory; open circles: KPNO. Zero phase is a time of periastron passage.

Table 5
Model Atmosphere Parameters and Iron Abundances

HD	T_{eff} (K)	log g (cgs)	v_t (km s^{-1})	[Fe/H]	σ	Number of Lines
100167	5900	4.37	0.5	0.06	0.14	41
135991	6050	4.34	1.0	−0.17	0.16	34
140667	5950	4.52	1.1	−0.27	0.11	44
158222	5700	4.35	0.6	0.02	0.18	40
217924	5900	4.53	0.5	−0.12	0.18	45

Table 6
Iron Abundance Comparison

HD	Holmberg et al. (2007)		This Work	
	T_{eff} (K)	[Fe/H]	T_{eff} (K)	[Fe/H]
100167	5728	−0.05	5900	0.06
135991	5929	−0.20	6050	−0.17
140667	5768	−0.35	5950	−0.27
158222	5598	−0.13	5700	0.02
217924	5702	−0.34	5900	−0.12

Table 7
Radial Velocities of HD 100167

Hel. Julian Date (−2400000)	Phase	Rad. Vel. (km s^{-1})	$(O - C)$ (km s^{-1})	Source[a]
52330.948	0.502	−28.0	0.3	KPNO
52707.856	0.724	−22.4	0.1	KPNO
52708.842	0.740	−22.0	−0.2	KPNO
52759.791	0.581	−26.6	0.2	KPNO
53120.734	0.539	−27.4	0.3	KPNO
53171.678	0.380	−29.6	0.1	KPNO
53491.705	0.663	−24.5	0.2	KPNO
53532.642	0.338	−29.9	0.1	KPNO
53536.648	0.404	−29.6	−0.1	KPNO
53850.791	0.590	−26.5	0.1	KPNO
54130.025	0.199	−29.1	0.1	Fair

Note. [a] KPNO = Kitt Peak National Observatory; Fair = Fairborn Observatory.

(This table is available in its entirety in machine-readable and Virtual Observatory (VO) forms in the online journal. A portion is shown here for guidance regarding its form and content.)

8.2. HD 135991 = HIP 74821

8.2.1. Brief History

Nordström et al. (2004) also included HD 135991 [$\alpha = 15^h17^m27^s\!\!.62$ $\delta = 22°17'59''\!\!.5$ (2000)] in their Geneva–Copenhagen survey of solar neighborhood stars. From four spectrograms they determined its radial velocity to be −22.1 km s^{-1}. Robinson et al. (2007) observed the star as part of an extensive low-resolution spectroscopic survey for metal-rich planet-search targets. From several calibrated spectral indices they found HD 135991 to have [Fe/H] = −0.13, while the photometric calibration of Holmberg et al. (2007) produced [Fe/H] = −0.20.

8.2.2. Orbital Analysis

Orbital phase coverage of both the 95 Fairborn and 34 KPNO radial velocities of HD 135991 is very good. Our separate solutions of the two data sets produced excellent agreement between all orbital elements, including the two center-of-mass velocities, which agreed to better than 0.1 km s^{-1}. We next computed a final joint solution in which all velocities were given unit weight. Our velocities are listed in Table 8, and the final orbital elements from the joint data solution are given in Table 2. Figure 2 provides a comparison of our velocities with the radial velocity curve computed from the final orbital elements.

8.1.3. Discussion

From a comparison with various reference stars we assign a spectral class of G0 to HD 100167, while the *Hipparcos* parallax and apparent magnitude (Table 1) combine to indicate that the star is a dwarf. The mass function, computed from the orbital elements, is 0.049 $M_{\odot}$, more than twice as large as that for any of the other four binaries. Such a value is large enough to suggest that lines of the secondary might be visible at red wavelengths (e.g., Stockton & Fekel 1992). However, upon careful examination of our Fairborn and KPNO spectra, no lines of a secondary were detected, indicating that the magnitude difference between the components is greater than 2.5 (Stockton & Fekel 1992).

From a calibration of Ca II H and K emission measurements Wright et al. (2004) obtained a rotation period of 16 days compared with our pseudosynchronous period of 10.4 days. With the basic parameters in Table 1 we obtain a radius of 1.08 $R_{\odot}$ from the Stefan–Boltzmann relation. Then the 16 day period results in a rotational velocity of 3.4 km s^{-1}, while the shorter pseudosynchronous period produces a larger velocity of 5.3 km s^{-1}. The measured $v \sin i$ value of 4 km s^{-1}, averaged from our result and two other independent determinations (Nordström et al. 2004; Valenti & Fischer 2005), is intermediate between the two predictions.
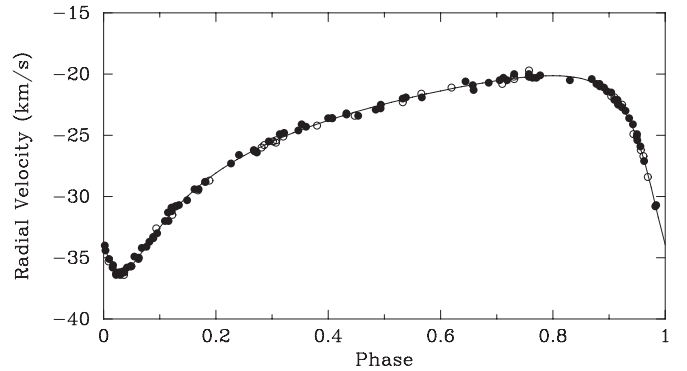
Table 8
Radial Velocities of HD 135991

Hel. Julian Date (−2400000)	Phase	Rad. Vel. (km s⁻¹)	(O − C) (km s⁻¹)	Source[a]
52392.889	0.619	−21.1	0.1	KPNO
52757.857	0.036	−36.4	−0.2	KPNO
52759.839	0.049	−35.7	0.0	KPNO
53121.900	0.447	−23.4	−0.3	KPNO
53168.803	0.758	−20.2	0.0	KPNO
53492.873	0.904	−21.8	−0.2	KPNO
53532.786	0.168	−29.5	−0.3	KPNO
53535.824	0.188	−28.7	−0.2	KPNO
53851.874	0.281	−26.0	−0.1	KPNO
54003.590	0.286	−25.8	0.0	KPNO
54221.797	0.731	−20.4	−0.1	KPNO
54246.744	0.896	−21.4	−0.1	Fair

Note. [a] KPNO = Kitt Peak National Observatory; Fair = Fairborn Observatory.

(This table is available in its entirety in machine-readable and Virtual Observatory (VO) forms in the online journal. A portion is shown here for guidance regarding its form and content.)

8.2.3. Discussion

Our spectral class is F9 and the *Hipparcos* parallax and apparent magnitude from Table 1 combine to identify the star as a dwarf. We determine a $v \sin i$ value of 6.7 km s⁻¹ in reasonable agreement with the value of 8 km s⁻¹ found by Nordström et al. (2004). Of our five binaries HD 135991 has the largest projected rotational velocity and the second shortest pseudosynchronous rotation period, 41.8 days. From the Stefan–Boltzmann relation we adopt a radius of 1.17 $R_\odot$. The period and radius result in a pseudosynchronous rotational velocity of 1.4 km s⁻¹, while HD 135991 is actually rotating at least five times more rapidly.

8.3. HD 140667 = HIP 77098

8.3.1. Brief History

HD 140667 [$\alpha = 15^h44^m31\overset{s}{.}86$ $\delta = 11°15'59\overset{''}{.}4$ (2000)] was classified by Harlan & Taylor (1970) as a G0 V star. Olsen (1994) obtained Strömgren photometry of it, and Nordström et al. (2004) included it in the Geneva–Copenhagen survey of stars in the solar neighborhood. From three observations their average radial velocity is −16.7 km s⁻¹.

8.3.2. Orbital Analysis

We acquired 123 Fairborn and 25 KPNO radial velocities of HD 140667, and both sets of observations provide good coverage of the orbital phases. The orbital elements from individual solutions of the two data sets are in very good agreement, with the two center-of-mass velocities differing by less than 0.1 km s⁻¹. All observations were given unit weights in a final solution of the combined data. Table 9 lists our velocity observations, and the orbital elements from our combined solution are given in Table 2. The radial velocities and the radial velocity curve from our orbital elements are shown in Figure 3.

8.3.3. Discussion

From our red wavelength spectra we determine a spectral class of F9 for HD 140667. Its *Hipparcos* parallax and apparent magnitude (Table 1) lead us to the conclusion that the star
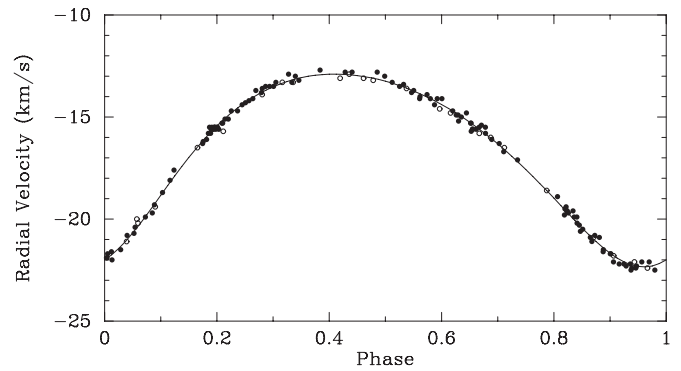

Figure 3. Radial velocities of HD 140667 compared with the computed velocity curve. Dots: Fairborn Observatory; open circles: KPNO. Zero phase is a time of periastron passage.

Table 9
Radial Velocities of HD 140667

Hel. Julian Date (−2400000)	Phase	Rad. Vel. (km s⁻¹)	(O − C) (km s⁻¹)	Source[a]
52706.010	0.616	−14.8	−0.2	KPNO
52755.944	0.667	−15.8	−0.2	KPNO
53119.928	0.039	−21.1	−0.1	KPNO
53169.792	0.090	−19.4	−0.2	KPNO
53491.880	0.419	−13.1	−0.2	KPNO
53532.809	0.461	−13.1	−0.1	KPNO
53851.895	0.787	−18.6	0.0	KPNO
53904.689	0.841	−20.2	0.0	Fair
53927.726	0.865	−20.9	−0.1	Fair
53998.650	0.937	−22.5	−0.3	Fair

Note. [a] KPNO = Kitt Peak National Observatory; Fair = Fairborn Observatory.

(This table is available in its entirety in machine-readable and Virtual Observatory (VO) forms in the online journal. A portion is shown here for guidance regarding its form and content.)

is a dwarf. Our classification is in close agreement with the G0 V spectral type of Harlan & Taylor (1970). We measure a $v \sin i$ value of 2.3 km s⁻¹ compared with a value of 4 km s⁻¹ by Nordström et al. (2004). HD 140667 has the longest pseudosynchronous rotation period of our five binaries, 782 days, resulting in a predicted pseudosynchronous rotational velocity of less than 0.1 km s⁻¹, and so this star, although rotating slowly, is clearly rotating faster then its pseudosynchronous rate.

8.4. HD 158222 = HIP 85244

8.4.1. Brief History

Like HD 100167, Nidever et al. (2002) observed HD 158222 [$\alpha = 17^h25^m08\overset{s}{.}32$ $\delta = 53°07'57\overset{''}{.}9$ (2000)] in a velocity survey of late-type stars. From three observations they found it to have a variable velocity with an average of −14.3 km s⁻¹. This value is very different from the average value of −27.5 km⁻¹ found by Nordström et al. (2004).

Based on a comparison with a grid of stellar evolutionary tracks, Holmberg et al. (2009) determined an age of 10.2 Gyr for HD 158222. Wright et al. (2004) obtained Ca II H and K emission measurements from high resolution spectra and used a chromospheric activity calibration to determine a much younger age of 4.1 Gyr, while the more recent activity–age calibration of Mamajek & Hillenbrand (2008, their Equation (3)) increases the age to 4.9 Gyr.
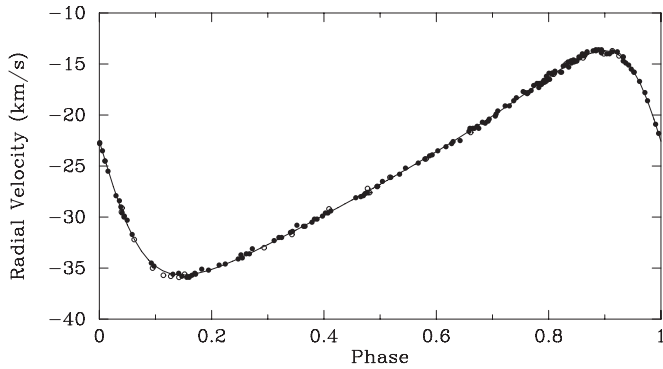
Figure 4. Radial velocities of HD 158222 compared with the computed velocity curve. Dots: Fairborn Observatory; open circles: KPNO. Zero phase is a time of periastron passage.

8.4.2. Orbital Analysis

With 152 Fairborn Observatory radial velocities all phases of the moderately eccentric orbit of HD 158222 are well sampled. Although the 25 KPNO velocities do not cover a small phase region around periastron passage, they still produce a good orbit. Indeed, the orbital elements of the Fairborn and KPNO solutions are in excellent agreement, and in particular, the center-of-mass velocities differ by less than 0.1 km s^{-1}. With weights of 1.0 for the Fairborn velocities and 0.7 for the KPNO velocities, a solution of the combined data sets was obtained. Table 10 lists our velocity observations, and the final orbital elements are given in Table 2. Figure 4 compares the radial velocities and the radial velocity curve from our orbital elements.

8.4.3. Discussion

Comparing the spectrum of HD 158222 with those of various reference stars of known spectral type, we classify it as G5 V. Our $v \sin i$ value of 2.2 km s^{-1} is in excellent agreement with the value of 2 km s^{-1} from Nordström et al. (2004). The pseudosynchronous rotation period for HD 158222 is 97 days, and from the Stefan–Boltzmann relation we estimate a radius of 1.09 $R_\odot$. Those values result in a pseudosynchronous rotational velocity of 0.6 km s^{-1}, and so HD 158222, although slowly rotating, is rotating faster than that value.

8.5. HD 217924 = HIP 113884

8.5.1. Brief History

Harlan & Taylor (1970) classified HD 217924 [$\alpha = 23^h03^m50\overset{s}{.}59 \, \delta = 21°35'53\overset{''}{.}8$ (2000)] as G0 V. Like the previous four binaries Nordström et al. (2004) included HD 217924 in their extensive survey of solar neighborhood stars. From three Coravel observations they found an average velocity of 19.1 km s^{-1} but with a standard deviation of 3.8 km s^{-1}. They concluded from the velocity variations that HD 217924 is a spectroscopic binary. They also estimated [Fe/H] = -0.34 and $v \sin i = 3$ km s^{-1}. As a result of a comparison of the *Hipparcos* and *Tycho-2* proper motions, Frankowski et al. (2007) also flagged it as a binary.

8.5.2. Orbital Analysis

Given the very large eccentricity of its orbit, the phase coverage, and the small number of orbital cycles that have been observed, there are two possible periods for HD 217924, 2648 and 2403 days, depending on whether the first KPNO velocity is placed on the descending or ascending part of the velocity
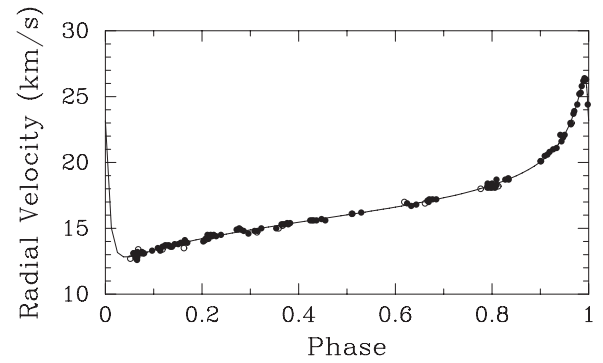

Figure 5. Radial velocities of HD 217924 compared with the computed velocity curve. Dots: Fairborn Observatory; open circles: KPNO. Zero phase is a time of periastron passage.

Table 10
Radial Velocities of HD 158222

Hel. Julian Date (-2400000)	Phase	Rad. Vel. (km s^{-1})	$(O - C)$ (km s^{-1})	Source[a]
52538.647	0.409	-29.2	0.3	KPNO
52758.966	0.478	-27.6	-0.1	KPNO
53171.800	0.481	-27.6	-0.2	KPNO
53492.910	0.039	-29.5	-0.2	KPNO
54003.630	0.517	-26.1	0.1	KPNO
54222.889	0.581	-24.3	-0.1	KPNO
54238.685	0.658	-21.6	0.0	Fair
54240.686	0.668	-21.3	0.0	Fair
54241.686	0.673	-21.1	0.0	Fair
54251.963	0.722	-19.1	0.2	Fair

Note. [a] KPNO = Kitt Peak National Observatory; Fair = Fairborn Observatory.

(This table is available in its entirety in machine-readable and Virtual Observatory (VO) forms in the online journal. A portion is shown here for guidance regarding its form and content.)

curve, respectively. With the longer period all the other KPNO velocities that were obtained before the Fairborn observations were begun have large systematic residuals from the orbital fit. Comparing the velocity residuals for orbits with the above two periods, the sum of the weighted square of the residuals decreases by 45% for the orbit with the shorter period. Thus, we have identified the period of 2403 days or 6.6 yr as the correct one. This period is by far the longest of the five binaries that we have analyzed.

Our 109 Fairborn velocities nearly cover one orbital period and are well distributed in phase except for the very rapid nodal passage, which mostly took place when HD 217924 was behind the Sun. Fortunately, two observations were obtained after the star began its rapid velocity change from maximum to minimum velocity, significantly constraining the orbital elements. The 17 KPNO velocities extend over nearly 1.5 orbital cycles and provide moderately good orbital phase coverage, but unfortunately, they completely miss the maximum velocity peak and the rapid velocity decline through periastron passage. As a result, those velocities by themselves do not enable the orbital solution of the elements to converge. However, adopting the elements from the Fairborn velocities results in an excellent orbital solution of the KPNO velocities. The two sets of velocities are listed in Table 11. With weights of 1.0 and 0.3 for the Fairborn and KPNO velocities, respectively, these data produce the orbital solution given in Table 2. Our radial velocities and the computed radial velocity curve are compared in Figure 5.

Table 11
Radial Velocities of HD 217924

Hel. Julian Date (−2400000)	Phase	Rad. Vel. (km s^{-1})	(O − C) (km s^{-1})	Source[a]
52540.820	0.901	20.1	0.0	KPNO
52902.791	0.052	12.7	−0.1	KPNO
52941.726	0.068	13.4	0.4	KPNO
53168.985	0.162	13.5	−0.4	KPNO
53273.772	0.206	14.1	−0.2	KPNO
53531.966	0.314	14.7	−0.3	KPNO
53639.786	0.358	15.0	−0.2	KPNO
54003.751	0.510	16.1	0.0	KPNO
54006.771	0.511	16.1	0.0	Fair
54050.649	0.529	16.2	0.0	Fair

Note. [a] KPNO = Kitt Peak National Observatory; Fair = Fairborn Observatory.

(This table is available in its entirety in machine-readable and Virtual Observatory (VO) forms in the online journal. A portion is shown here for guidance regarding its form and content.)

8.5.3. Discussion

Our spectral type for HD 217924 is G2 V, in reasonable accord with the G0 V type of Harlan & Taylor (1970). Our projected rotational velocity of 2.2 km s^{-1} is similarly consistent with the value of 3 km s^{-1} determined by Nordström et al. (2004). Despite its 6.6 yr orbital period, the orbital eccentricity of HD 217924 is so large, 0.84, that the pseudosynchronous rotation period is just 132 days. Nevertheless, such a period is long enough that like all but one of the other solar-type stars in this work, HD 217924 is rotating faster than its pseudosynchronous velocity.

REFERENCES

Barker, E. S., Evans, D. S., & Laing, J. D. 1967, RGOB, 130, 355
Bopp, B. W., Evans, D. S., Laing, J. D., & Deeming, T. J. 1970, MNRAS, 147, 355
Bubar, E. J., & King, J. R. 2010, AJ, 140, 293
Carpenter, J. M., Bouwman, J., Mamajek, E. E., et al. 2009, ApJS, 181, 197
Casagrande, L., Schönrich, R., Asplund, M., et al. 2011, A&A, 530, A138
Castelli, F., & Kurucz, R. L. 2003, in IAU Symp. 210, Modelling of Stellar Atmospheres, ed. N. Piskunov, W. W. Weiss, & D. F. Gray (San Francisco, CA: ASP), Poster A20 on Enclosed CD-ROM
Duquennoy, A., & Mayor, M. 1991, A&A, 248, 485
Eaton, J. A., & Williamson, M. H. 2004, SPIE, 5496, 710
Eaton, J. A., & Williamson, M. H. 2007, PASP, 119, 886
Fekel, F. C. 1997, PASP, 109, 514
Fekel, F. C., Tomkin, J., & Williamson, M. H. 2009, AJ, 137, 3900
Frankowski, A., Jancart, S., & Jorissen, A. 2007, A&A, 464, 377
Harlan, E. A., & Taylor, D. C. 1970, AJ, 75, 165
Henry, G. W. 1999, PASP, 111, 845
Holmberg, J., Nordström, B., & Andersen, J. 2007, A&A, 475, 519
Holmberg, J., Nordström, B., & Andersen, J. 2009, A&A, 501, 941
Hut, P. 1981, A&A, 99, 126
Mamajek, E. E., & Hillenbrand, L. A. 2008, ApJ, 687, 1264
Nidever, D. L., Marcy, G. W., Butler, R. P., Fischer, D. A., & Vogt, S. S. 2002, ApJS, 141, 503
Nordström, B., Mayor, M., Andersen, J., et al. 2004, A&A, 418, 989
Olsen, E. H. 1994, A&AS, 106, 257
Perryman, M. A. C., & ESA 1997, The *Hipparcos* and *Tycho* Catalogues (ESA SP-1200; Noordwijk: ESA)
Robinson, S. E., Ammons, S. M., Kretke, K. A., et al. 2007, ApJS, 169, 430
Scarfe, C. D. 2010, Obs, 130, 214
Sneden, C. 1973, ApJ, 184, 839
Stockton, R. A., & Fekel, F. C. 1992, MNRAS, 256, 575
Strassmeier, K. G., & Fekel, F. C. 1990, A&A, 230, 389
Takeda, G., Ford, E. B., Sills, A., et al. 2007, ApJS, 168, 297
Tassoul, J.-L., & Tassoul, M. 1992, ApJ, 395, 259
Valenti, J. A., & Fischer, D. A. 2005, ApJS, 159, 141
van Leeuwen, F. 2007, A&A, 474, 653
White, R. J., Gabor, J. M., & Hillenbrand, L. A. 2007, AJ, 133, 2524
Wolfe, R. H., Horak, H. G., & Storer, N. W. 1967, in Modern Astrophysics, ed. M. Hack (New York: Gordon & Breach), 251
Wright, J. T., Marcy, G. W., Butler, R. P., & Vogt, S. S. 2004, ApJS, 152, 261
Zahn, J.-P. 1977, A&A, 57, 383